





# Gastric-stable multiple emulsions for delivery of chemopreventive agents

Agnieszka Markowska-Radomska<sup>\*1</sup> , Ewa Dluska<sup>1</sup> , Elzbieta Gorska-Horczyzak<sup>2</sup> ,  
Magdalena Zalewska<sup>2</sup> 

<sup>1</sup> Warsaw University of Technology, Faculty of Chemical and Process Engineering, Warsaw, Poland

<sup>2</sup> Warsaw University of Life Sciences, Institute of Human Nutrition Sciences, Department of Technique and Food Development, Warsaw, Poland

## Abstract

This study investigates multiple emulsions as structured, food-grade delivery systems of chemopreventive agents designed to improve the stability and gastric protection of functional compounds. Emulsions were prepared using a Couette–Taylor flow contactor, enabling precise control over droplet size and internal architecture. Sodium carboxymethyl cellulose (CMC) was employed as a multifunctional stabilising agent. The presence of CMC significantly improved droplet integrity, encapsulation efficiency, and long-term physical stability. Furthermore, CMC acted as an oxygen barrier, increasing the oxidative stability of the membrane oil phase. Under simulated gastric conditions, the emulsions demonstrated controlled release behaviour influenced by both droplet structure and CMC concentration. Systems with smaller droplets and higher CMC levels exhibited slower release rates of both lipophilic (resveratrol) and hydrophilic (selenium) compounds, especially during the first two hours of gastric exposure. These observations suggest that increased viscosity and interfacial structuring contribute to delayed diffusion and improved compound retention in acidic environments. The release-modulating effects were particularly evident in emulsions with higher surface area and CMC concentration. Integrating tunable droplet design with hydrocolloid functionality offers a promising route to enhancing physical stability and release control. This approach supports the development of fortified emulsions with chemopreventive agents for functional food and nutraceutical applications requiring targeted delivery and protection during gastric transit.

\* Corresponding author, e-mail:  
[agnieszka.markowska@pw.edu.pl](mailto:agnieszka.markowska@pw.edu.pl)

## Article info:

Received: 03 June 2025

Revised: 16 July 2025

Accepted: 18 July 2025

## Keywords

multiple emulsion, chemoprevention, drug delivery system, mass transfer process, hydrocolloid stabiliser

## 1. INTRODUCTION

The growing interest in health-oriented diets has spurred the development of functional food systems designed to address micronutrient deficiencies, support physiological resilience, and reduce the burden of chronic diseases. Particular attention has been directed towards incorporating bioactive compounds with chemopreventive potential, including anti-inflammatory agents, metabolic regulators, antioxidants, and essential micronutrients (Katona and Weiss, 2020). Among these, trans-resveratrol and selenium have attracted particular interest due to their proven ability to reduce the risk of colorectal cancer, a malignancy associated with poor prognosis and high mortality (Ashique et al., 2024). Trans-resveratrol, a natural polyphenol, suppresses tumour progression by modulating key signalling pathways such as NF- $\kappa$ B and Wnt/ $\beta$ -catenin (Wang et al., 2020). Selenium enhances cancer prevention by promoting apoptosis and the generation of reactive oxygen species (ROS) (Majumdar et al., 2009). The combined use of trans-resveratrol and selenium has demonstrated greater efficacy than individual administration (Zhuang et al., 2020).

Despite their health benefits, the integration of such chemopreventive agents into food systems is limited by their poor aqueous solubility, chemical instability, and susceptibility to

degradation during gastrointestinal transit (Islam et al., 2024; Wang et al., 2023). Furthermore, these compounds can adversely affect the sensory properties of foods, reducing consumer acceptance. Consequently, food-grade delivery systems must ensure compound stability, controlled release, sensory acceptability, dietary compatibility, and facilitate incorporation into a wide range of food products.

In response to these challenges, various food-grade delivery systems have been developed, including pH-responsive coatings (Li et al., 2022), hydrocolloid-based matrices (Sheng et al., 2021), and lipid-based carriers such as liposomes, nanoemulsions, solid lipid nanoparticles (SLNs), and nanostructured lipid carriers (NLCs) (Fathi et al., 2019; Liu et al., 2024; Lu et al., 2021; Mall et al., 2025). Among these, multiple water-in-oil-in-water (W/O/W) emulsions have received increasing attention due to their unique structure, enabling the simultaneous encapsulation of hydrophilic and lipophilic compounds. This architecture enhances stability, bioavailability, and protection of encapsulated agents against gastric degradation (Li et al., 2024) while allowing modulation of release kinetics (Dluska et al., 2022). Consequently, W/O/W emulsions support continuous delivery of functional components and more balanced intake. Their advantages have led to growing interest in pharmaceutical, clinical, and food-related fields



(Dluska et al., 2019; Lu et al., 2016; Markowska-Radomska et al., 2021; McClements et al., 2007). Nevertheless, the inherent instability of multiple emulsions, manifested by phase separation, droplet coalescence, and flocculation, remains a significant barrier to practical application (Huang et al., 2023).

Various agents have been investigated to improve the stability of multiple emulsions. Among them, sodium carboxymethyl cellulose (CMC) is receiving particular attention (Cook et al., 2018). CMC, a biocompatible, food-grade polysaccharide, enhances emulsion stability by preventing phase separation and droplet aggregation (Wang et al., 2024), while its mucoadhesive properties may promote prolonged intestinal retention and improved bioavailability. The protective network that forms around emulsified droplets (Jia et al., 2015) further supports controlled release of encapsulated bioactives. Owing to its neutral flavour and versatility across food systems, CMC facilitates integration into routine dietary formats, contributing to adherence to long-term pro-health interventions. Nevertheless, a deeper understanding of how CMC modulates multiple emulsions' physicochemical properties and gastrointestinal behaviour remains essential for developing stable and effective carriers for chemopreventive compounds in functional foods.

Recent studies emphasise the critical role of hydrocolloid–interface interactions and emulsion microstructure in designing effective delivery systems for functional foods. Multiple

emulsions stabilised with CMC offer promising opportunities for the encapsulation and controlled release of chemopreventive agents, supporting the development of advanced health-promoting food matrices.

The objective of this study was to develop and characterise a CMC-stabilised W/O/W multiple emulsion system for the delivery of trans-resveratrol and selenium (Figure 1). To obtain well-defined droplet architecture, emulsions were prepared using a Couette–Taylor flow contactor. By combining the protective architecture of multiple emulsions with the functional benefits of CMC, the system aims to achieve enhanced stability, targeted intestinal delivery, and controlled release.

Sesame oil, used as the membrane phase in this study, is rich in unsaturated fatty acids and bioactive compounds such as sesamin and sesamol, which possess antioxidant properties known to reduce oxidative stress and inflammation, key factors in colorectal cancer development (Namiki, 2007). It stabilises cell membranes and modulates lipid metabolism, reinforcing its potential chemopreventive role. However, maintaining the oxidative stability of oil is critical, as degradation of bioactive compounds or alteration of fatty acid profiles may diminish its protective properties. Notably, lipid oxidation is generally more pronounced in emulsions due to their increased interfacial area and oxygen exposure and is further influenced by emulsifier composition, processing

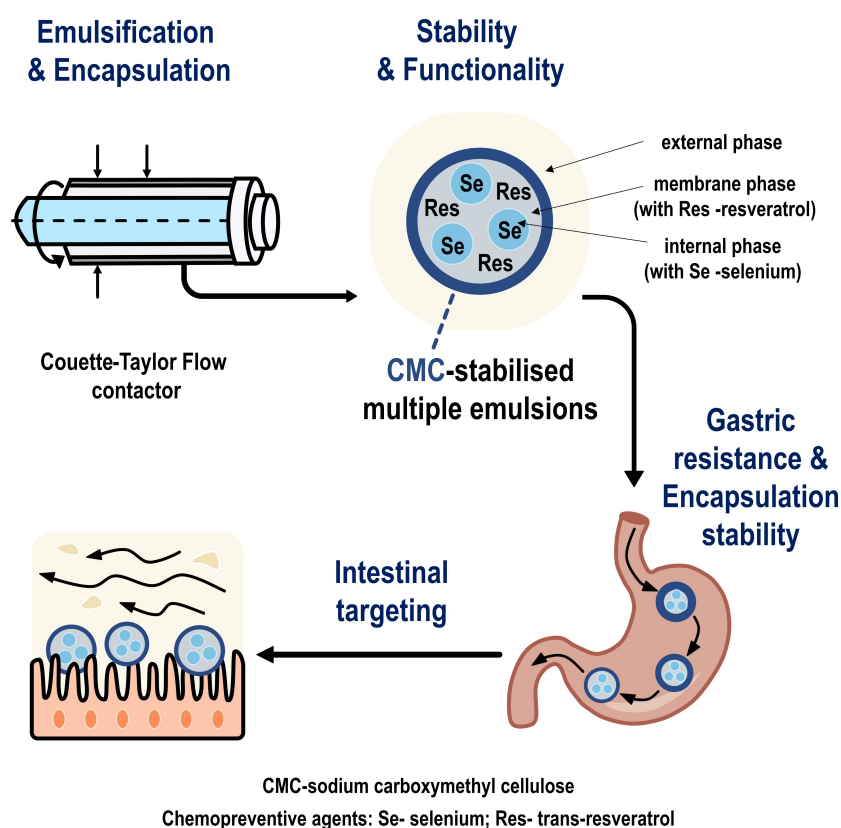


Figure 1. Schematic representation of the multiple emulsion-based carrier prepared using a Couette–Taylor flow contactor, combining the protective structure of multiple emulsions with the functional properties of CMC, resulting in enhanced gastric resistance, improved structural and encapsulation stability, and targeted intestinal delivery.

conditions, and component interactions (McClements and Decker, 2000). The developed emulsions were characterised in terms of physicochemical properties, droplet size distribution, interfacial behaviour, rheology, and release kinetics under simulated gastrointestinal conditions.

## 2. MATERIALS AND METHODS

### 2.1. Materials

Emulsifying and stabilising agents: Pluronic P123, Span 83, and sodium carboxymethyl cellulose (CMC, high viscosity) were supplied by Sigma–Aldrich GmbH (Germany), powdered gelatin, pure p.a. (Avantor, Poland), while Tween 80 was obtained from Fisher Scientific Company L.L.C. Active compounds: trans-resveratrol, selenium were supplied by Sigma–Aldrich (Poland). Enzymes:  $\alpha$ -amylase from human saliva (Type IX-A, 1000–3000 U·mg<sup>−1</sup> protein), pepsin from porcine gastric mucosa (3200–4500 U·mg<sup>−1</sup> protein) (Sigma–Aldrich, Poland). Refined sesame oil (Caesar & Loretz GmbH, Germany). Chemicals: sodium bicarbonate, sodium chloride, potassium chloride, calcium chloride dihydrate, monosodium phosphate, ammonium carbonate, magnesium chloride hexahydrate, hydrochloric acid (1 M), chloroform, methanol, phenol (85%), ethanol (50%), and sulphuric acid (96%) were purchased from Avantor (Poland). Other reagents: phosphate buffer (PBS), 2-mercaptobenzothiazole, and the Supelco 37 Component FAME mix were obtained from Sigma–Aldrich (Poland). High-purity distilled water (Milli-Q water) was used. All solvents used for the analysis were of analytical grade.

### 2.2. Analytical methods for chemopreventive agent quantification

The concentrations of chemopreventive agents in the external emulsion phase (for encapsulation efficiency) and simulated gastric fluids (during release studies) were determined using substance-specific methods. A spectrophotometric method was used for resveratrol (Camont et al., 2009). Absorbance was measured at 305 nm. Sample concentrations were determined by comparing absorbance values with the calibration curves. Selenium in the samples was measured separately, following Bera and Chakrabarty (1968). The sample pH was adjusted to  $7.5 \pm 0.2$  using HCl/NaOH (0.1 M) to optimise the formation of a yellow selenium complex with 2-mercaptobenzothiazole. For analysis, 1 cm<sup>3</sup> of the sample or standard solution was mixed with 15 cm<sup>3</sup> of 12 M HCl and 4 cm<sup>3</sup> of 0.1 g of 2-mercaptobenzothiazole per 100 cm<sup>3</sup> of 50% ethanol. The mixture was diluted with 2 M HCl and left for 10 minutes at room temperature, and absorbance was measured at 370 nm against a reagent blank. Selenium concentration was determined via a calibration curve. All measurements were performed using a spectrophotometer Jasco, Model FP-6500.

### 2.3. Preparation of multiple emulsions

Multiple emulsions were prepared using a one-step emulsification process described in our previous work (Dluska et al., 2017; Dluska et al., 2019; Markowska-Radomska and Dluska, 2012). A Couette–Taylor flow (CTF) liquid-liquid contactor in a horizontal position was used for emulsification and simultaneous encapsulation of bioactive substances. Emulsification occurred in the concentric annular gap between the inner rotating and outer stationary cylinders (inner diameter: 0.035 m, gap width: 1.5 mm, length: 0.4 m). Two emulsion Sets (I and II) with different oil phase contents were prepared, each varying in initial sodium carboxymethyl cellulose (CMC) concentration (0.0, 0.1, 0.3, and 0.5 wt.%) in the external phase. Preparation conditions ensured consistent membrane droplet diameters within each set despite differences in CMC content. Emulsions were prepared in triplicate. Table 1 summarises the phase compositions and emulsification conditions. The emulsions were stored in dark glass bottles at 25 °C to assess long-term physicochemical stability, including droplet size changes, encapsulation efficiency, and oxidative stability of the membrane phase.

The composition of chemopreventive agents in 100 cm<sup>3</sup> of emulsion: 1.5 mg trans-resveratrol (228.25 g·mol<sup>−1</sup>) and 55 µg selenium (78.97 g·mol<sup>−1</sup>). Lipophilic resveratrol was encapsulated in sesame oil drops (membrane phase), while hydrophilic selenium was in the droplets of the aqueous internal phase.

### 2.4. Emulsion size, structure and stability: microscopy-based assessment

An Olympus BX60 microscope with an SC50 digital camera (Olympus, Japan) was used to examine multiple emulsion morphology. A thin emulsion layer was applied to microscope slides without a cover glass. The structure was analysed from a representative selection of images (Dluska et al., 2017; Dluska et al., 2019). Droplet size was determined using Image-Pro Plus 4.5 (Media Cybernetics, USA) via the three-point measurement method. Mean (Sauter) droplet diameters and droplet size distribution were calculated. Details of the storage conditions and the parameters assessed during the stability tests are described in Section 2.3.

### 2.5. Encapsulation efficiency measurements

To determine encapsulation efficiencies of trans-resveratrol (EER) and selenium (EES) in emulsions, the free (non-encapsulated) active agents in the continuous phase of the emulsion were quantified using methods from Section 2.2. The dispersed phase was separated via syringe filtration (regenerated cellulose, 0.45 µm, Profill, Czech Republic), which was selected based on preliminary evaluation and established practice in emulsified systems with similar droplet sizes, to ensure

Table 1. The composition and preparation conditions of emulsions in the Couette–Taylor flow contactor.

Emulsion phase composition						
Internal		gelatine 0.2 wt.%, Pluronic P-123 0.25 wt.%, Mili-Q water to 100 wt.%				
Membrane		sesame oil 98 wt.%, Span 83 2 wt.%				
External		sodium carboxymethyl cellulose-CMC: 0.0/0.1/0.3/0.5 wt.%, Pluronic P-123 0.25 wt.%, Tween 80 0.25 wt.%, Mili-Q water to 100 wt.%				
Preparation conditions						
		Rotational frequency rpm	Volumetric flow of the emulsion phases:			Volume fraction of dispersed phases ( $\phi$ )
			Internal $\text{cm}^3 \cdot \text{min}^{-1}$	Membrane $\text{cm}^3 \cdot \text{min}^{-1}$	External $\text{cm}^3 \cdot \text{min}^{-1}$	
Set I	MEI	900				
	MEI-CMC(0.1)	1200	30	30	60	0.5
	MEI-CMC(0.3)	1400				
	MEI-CMC(0.5)	1800				
Set II	MEII	1300				
	MEII-CMC(0.1)	1800				
	MEII-CMC(0.3)	2100	30	60	60	0.6
	MEII-CMC(0.5)	2450				

reliable separation without disrupting droplet integrity (Suñer et al., 2017). Encapsulation efficiency,  $EE$ , was calculated as the percentage of the total active ingredient entrapped in emulsion droplets (internal for selenium; membrane for resveratrol), (Eq. 1).

$$EE = (M_0 - M_t) \cdot M_0^{-1} \cdot 100\% \quad (1)$$

where:  $M_t$  – a mass of the non-encapsulated compound in the external phase at a given time;  $M_0$  – an initial compound mass added to the emulsion during preparation.

## 2.6. Rheological measurements

A RheolabQC rotational viscometer (Anton Paar, Austria) with a DG42 double-gap concentric cylinder system (gap length: 60 mm, size: 1.64 mm, cone angle/radius ratio:  $120^\circ/1.08$ ) was used to study emulsion rheology at shear rates of  $50\text{--}2500 \text{ s}^{-1}$ . Measurements were performed at  $37^\circ\text{C}$ .

## 2.7. Evaluation of oil phase oxidation under long-term storage

The fatty acid profiles of free sesame oil (bulk) and emulsified oil (membrane phase of emulsion) were analysed over 90 days. Samples were stored at  $25^\circ\text{C}$  in dark glass bottles ( $500 \text{ cm}^3$ ) sealed with aluminium caps with Teflon liners. In

the case of emulsified oil, before the analysis, the oil was extracted from emulsions using the Folch method (chloroform:methanol mixture–2:1 by volume) (Folch et al., 1957). Fatty acid methyl esters were synthesised directly. Analysis was performed using a Shimadzu GC-2010 gas chromatograph with a flame ionisation detector and an RT<sup>®</sup>-2560 column ( $100 \text{ m} \times 0.25 \text{ mm} \times 0.2 \mu\text{m}$ ). Helium was used as the carrier gas at  $1.0 \text{ cm}^3 \cdot \text{min}^{-1}$ . The temperature program was  $140^\circ\text{C}$  (5 min), increased at  $4^\circ\text{C} \cdot \text{min}^{-1}$  to  $240^\circ\text{C}$ , then held for 30 min. Injector and detector temperatures were  $240^\circ\text{C}$  and  $260^\circ\text{C}$ , respectively, with a 70:1 split ratio.

## 2.8. Simulated gastric condition

The gastric simulation followed a modified version of the protocol in Minekus et al. (2014), consisting of two phases: oral and gastric. In the oral phase,  $5 \text{ cm}^3$  of emulsion was mixed with  $3.5 \text{ cm}^3$  of simulated oral fluid (SOF),  $0.5 \text{ cm}^3$  of  $\alpha$ -amylase ( $1500 \text{ U} \cdot \text{cm}^{-3}$  in SOF),  $0.025 \text{ cm}^3$  of 0.3 M calcium chloride dihydrate, and  $0.975 \text{ cm}^3$  of distilled water. The pH was adjusted to 7 using 1 M HCl, and the mixture was incubated at  $37^\circ\text{C}$  for 2 minutes at 150 rpm in an orbital shaker. In the gastric phase,  $7.5 \text{ cm}^3$  of simulated gastric fluid (SGF),  $1.6 \text{ cm}^3$  of pepsin ( $25000 \text{ U} \cdot \text{cm}^{-3}$  in SGF),  $0.005 \text{ cm}^3$  of 0.3 M calcium chloride dihydrate, and  $0.695 \text{ cm}^3$  of distilled water were added. The pH was adjusted to 2 using 6 M HCl, and the mixture was incubated in amber  $25 \text{ cm}^3$  Falcon tubes



at 37°C, shaking at 150 rpm. Samples were incubated for up to 3 hours to simulate different gastric retention times. The compositions of the simulated oral and gastric phases are presented in Table 2.

Table 2. Formulations of the model fluids: simulated oral fluid (SOF) and simulated gastric fluid (SGF).

Salts	Stock concentration [M]	SOF $V_{SOF}^*$ [cm <sup>3</sup> ]	SGF $V_{SGF}^{**}$ [cm <sup>3</sup> ]
KCl	0.5	15.1	6.9
NaCl	1	–	11.8
KH <sub>2</sub> PO <sub>4</sub>	0.5	3.7	0.9
NaHCO <sub>3</sub>	1	6.8	12.5
MgCl <sub>2</sub> (H <sub>2</sub> O) <sub>6</sub>	0.15	0.5	0.4
(NH <sub>4</sub> ) <sub>2</sub> CO <sub>3</sub>	0.5	0.06	0.5
pH	–	7	2

\*, \*\* Volume of stock solution used to prepare 400 cm<sup>3</sup> of oral phase or gastric phase, respectively.

## 2.9. Emulsion morphology changes under gastric conditions

The morphology of emulsions under simulated gastric conditions was evaluated by analysing droplet size and distribution over different gastric retention times (1, 2 and 3 hours) relative to the initial value (0 h, immediately after preparation). Measurements followed the procedure in Section 2.4.

## 2.10. $\zeta$ -potential measurements

$\zeta$ -potential of the emulsions was determined using a Zetasizer Nano S series (Malvern Instruments, UK) and the DTS1070 capillary cell. The emulsions were diluted to 0.005 wt.% with PBS buffer at pH 2 (gastric conditions) to minimise multiple scattering effects. The measurements were conducted for up to 3 hours. The reference measurements were performed at pH7.

## 2.11. Mass transfer study in simulated gastric fluid

The release of resveratrol and selenium from emulsions was evaluated under simulated gastric conditions. Emulsions with varying CMC concentrations and droplet sizes were incubated at 37°C for up to 3 hours to mimic gastric retention (see Section 2.9). Samples were collected at set intervals, filtered (syringe filter, regenerated cellulose, 0.45  $\mu$ m, Profill, Czech Republic), and analysed to determine release profiles. Concentrations were measured using specific analytical methods (see Section 2.2). Results are presented as cumulative mass released over time relative to the initial encapsulated mass.

## 2.12. Statistical analysis

All data are presented as mean  $\pm$  standard deviation (SD). Experiments were performed in triplicate and analysed in triplicate unless stated otherwise. Lipid oxidation data were statistically analysed using Statistica 13 with one-way and two-way ANOVA, followed by Tukeys' HSD test where applicable. Differences were considered significant at  $p \leq 0.05$ .

# 3. RESULTS AND DISCUSSION

## 3.1. Initial characteristics of multiple emulsions

Two emulsion Sets, I and II, were prepared using a Couette–Taylor flow apparatus. Microscopic observations (Figure 2A) confirmed the formation of complex multiple (double) emulsions.

Regardless of the CMC concentration in the external phase, the emulsions of Set I predominantly exhibited single droplet-in-droplet structures, whereas Set II displayed multiple droplet-in-drop formations. As the CMC content increased, higher rotational speeds under preparation were required to maintain similar droplet sizes (Set I: 900–1800 rpm; Set II: 1300–2450 rpm). The initial droplet sizes and encapsulation efficiencies for each formulation are presented in Table 3.

Set II emulsions contained twice as much oil phase as Set I, resulting in approximately twice the size of membrane droplets, while internal phase droplets remained similar. The membrane phase droplet size in Set I ranged from 12.1  $\mu$ m (MEI) to 9.1  $\mu$ m (MEI-CMC(0.5)), while in Set II, it varied from 24.7  $\mu$ m (MEII) to 22.8  $\mu$ m (MEII-CMC(0.5)).

Encapsulation efficiencies of both chemopreventive agents were high for all formulations ( $EER > 91\%$ ;  $EES > 92\%$ ), with CMC-containing emulsions showing improved encapsulation content of active compounds compared to those without CMC. Additionally, Set II emulsions exhibited slightly higher encapsulation efficiencies than Set I for the same CMC content.

The viscosity measurements (Figure 2B) demonstrated that all emulsions exhibited non-Newtonian, shear-thinning pseudoplastic behaviour. Such rheological properties are highly desirable in oral administration, thereby ensuring effective and consistent administration, particularly for people with swallowing difficulties (Lavoisier et al., 2021).

Figure 2B shows that CMC addition significantly increases viscosity, particularly at higher concentrations (e.g. 0.5%) due to the thickening effect of CMC in the external phase, leading to formation of a structured aqueous phase that restricts droplet movement. Moreover, emulsions of Set II exhibit higher viscosity than Set I, reflecting its greater sesame oil

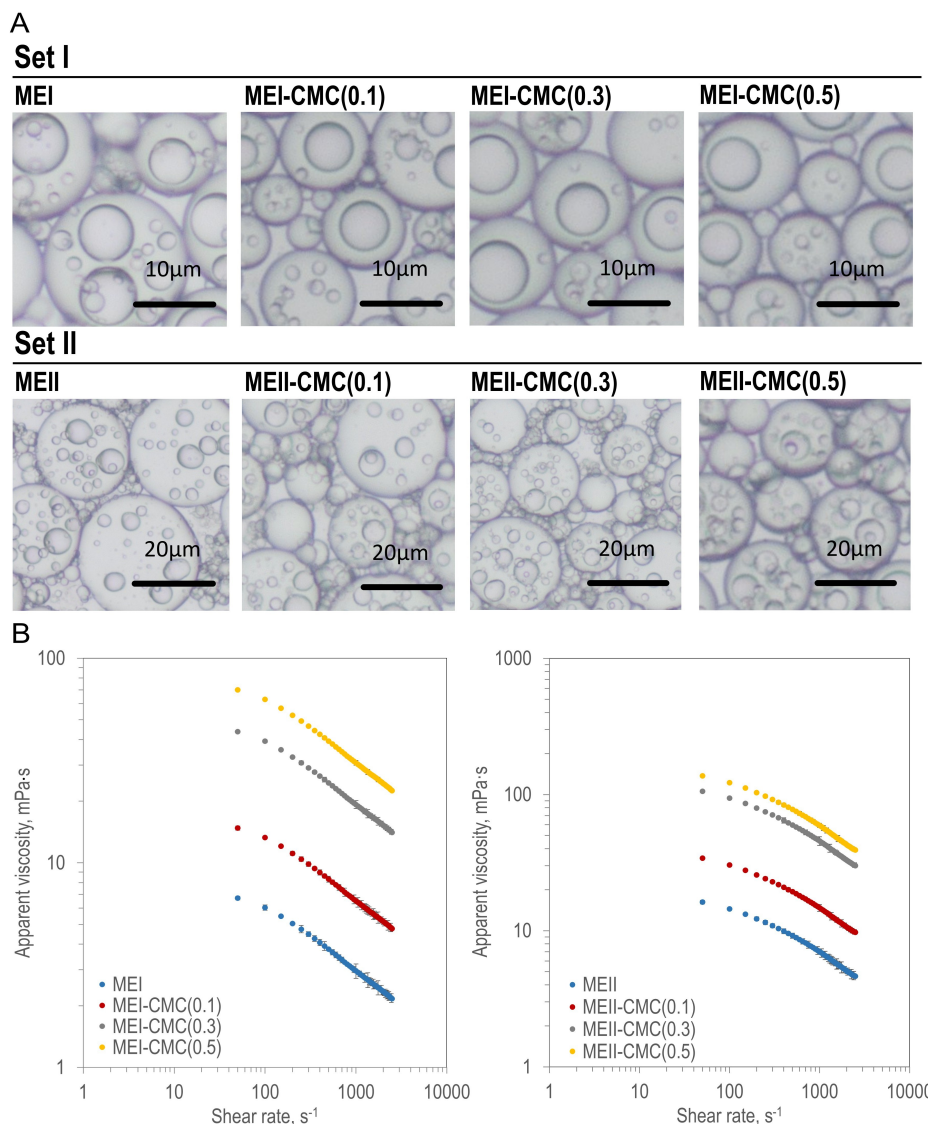


Figure 2. The initial characteristics of multiple emulsions with chemopreventive agents: (A) Optical microscope images, (B) Apparent viscosity as a function of the shear rate. All results are presented for emulsions with different sodium carboxymethyl cellulose (CMC) content (0–0.5 wt.%). Each value represents mean  $\pm$  SD, ( $n = 3$ ) (error bars are not visible when errors are equal to or smaller than the symbols for individual measurements).

Table 3. Initial characteristics of multiple emulsions.

Emulsion	$D_{32}^*$ µm	$d_{32}^*$ µm	$EER^{**}$ %	$EES^{**}$ %
MEI	$12.1 \pm 0.7$	$4.1 \pm 0.3$	$91.23 \pm 1.23$	$92.45 \pm 2.53$
Set I				
MEI-CMC(0.1)	$10.8 \pm 0.5$	$5.0 \pm 0.4$	$92.78 \pm 2.11$	$93.07 \pm 1.42$
MEI-CMC(0.3)	$9.4 \pm 0.3$	$4.2 \pm 0.3$	$93.18 \pm 1.21$	$94.18 \pm 0.21$
MEI-CMC(0.5)	$9.1 \pm 0.5$	$3.9 \pm 0.3$	$94.98 \pm 1.34$	$94.57 \pm 1.17$
MEII	$24.7 \pm 1.0$	$3.9 \pm 0.4$	$92.43 \pm 2.26$	$94.47 \pm 1.58$
Set II				
MEII-CMC(0.1)	$23.9 \pm 0.8$	$3.4 \pm 0.4$	$93.18 \pm 2.03$	$94.87 \pm 1.63$
MEII-CMC(0.3)	$23.3 \pm 0.6$	$3.6 \pm 0.3$	$95.45 \pm 1.44$	$95.87 \pm 0.97$
MEII-CMC(0.5)	$22.8 \pm 0.5$	$4.0 \pm 0.3$	$97.03 \pm 1.06$	$96.23 \pm 1.14$

\* $D_{32}$ ,  $d_{32}$  – the Sauter diameter of the membrane phase drops and internal phase droplets;

\*\* $EER$ ,  $EES$  – the encapsulation efficiencies of trans-resveratrol and selenium, respectively.

content (twice that of MEI), resulting in a higher volumetric fraction of dispersed phases in the system (Set II: 0.6 vs Set I: 0.5) and larger droplet size (Table 3). In addition, the results shown in Figure 2B demonstrate that the change in viscosity ( $\Delta\mu$ ) over the entire shear rate range ( $50\text{--}2500\text{ s}^{-1}$ ) is more pronounced within a given set of higher CMC concentrations. The effect is more evident for Set II (for CMC  $0.0 \rightarrow 0.5\text{ wt.}\%$  –  $\Delta\mu$  for Set I:  $4.6 \rightarrow 47.4\text{ mPa}\cdot\text{s}$  and Set II:  $11.6 \rightarrow 98.1\text{ mPa}\cdot\text{s}$ ). In contrast, Benchabane and Bekkour (2008) reported that the effect of aqueous carboxymethyl cellulose solutions (system without dispersed drops) was inverse concerning polymer concentration. The

results confirm that this pronounced effect stems from the interplay between the sesame oil phase and the thickening network formed by CMC in the aqueous phase.

### 3.2. Emulsion characteristics under storage conditions

#### 3.2.1. Structure and encapsulation stability of emulsions

The stability of the emulsions was evaluated by monitoring droplet size changes (Figure 3A) and encapsulation stability (Figure 3B) over 90 days at  $25^\circ\text{C}$ .

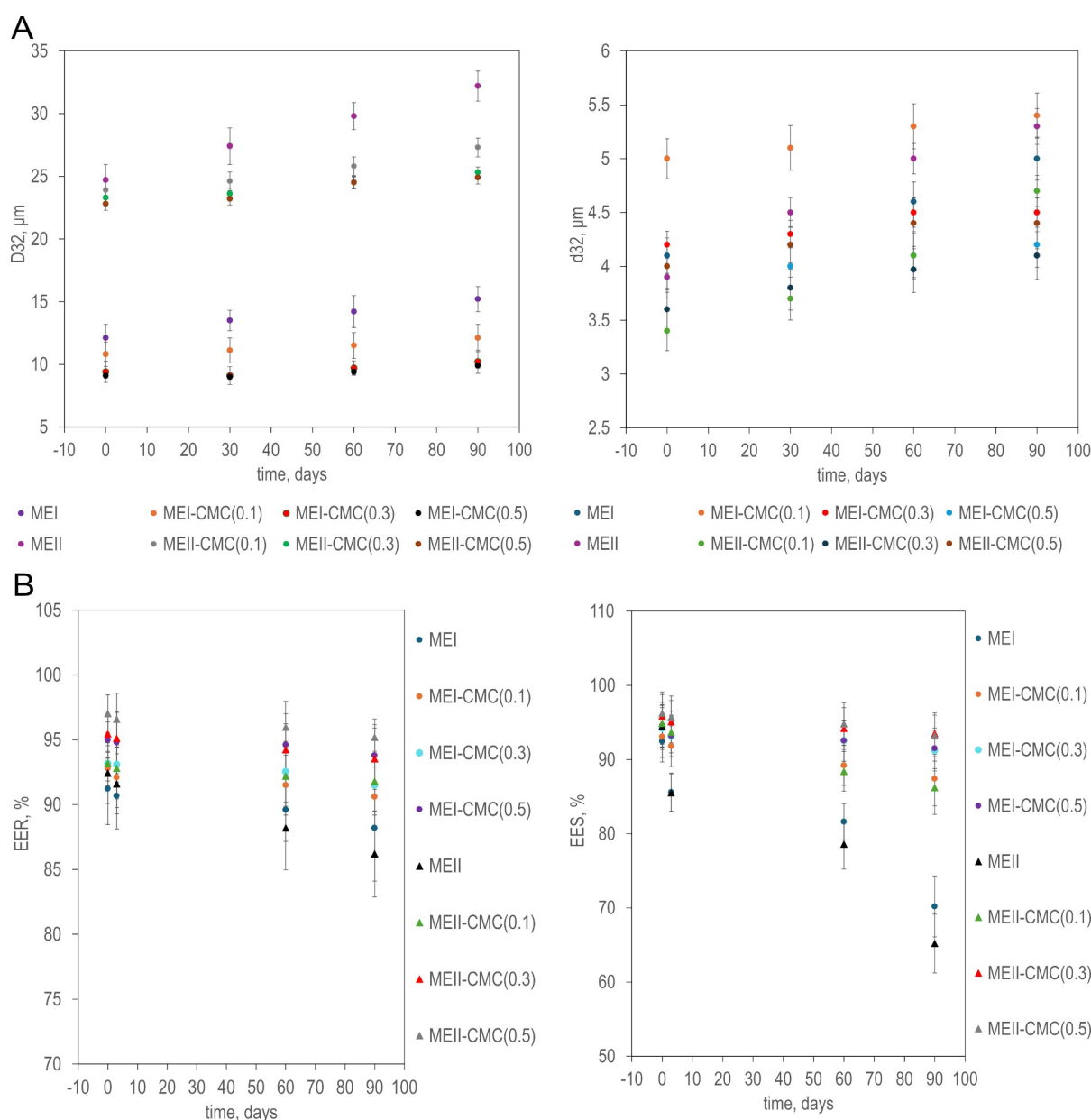


Figure 3. The behaviour of multiple emulsions with various sodium carboxymethyl cellulose content (0–0.5 wt.%) under storage conditions up to 90 days—changes in the drop size ( $D_{32}$ ,  $d_{32}$ —Sauter mean diameters of the membrane and internal phase drops, respectively): (A) encapsulation efficiencies of trans-resveratrol ( $EER$ ) and selenium ( $EES$ ) (B). Each value represents the mean  $\pm$  SD ( $n = 3$ ).

Emulsions with 0.5 wt.% CMC of Sets I, II showed minimal droplet size variations ( $\sim 10\%$ ), indicating high stability – those with 0.3 wt.% CMC exhibited slightly more significant changes (12–15%) but remained stable long-term. In contrast, emulsions without CMC (MEI, MEII) were the least stable, with membrane phase droplet size increases of 22–26% relative to the initial size of drops. The stabilising effect of CMC is further confirmed by the analysis of internal droplet size (Figure 3A). Emulsions with the highest CMC content (MEI-CMC(0.5), MEII-CMC(0.5)) showed minor changes in droplet size. In contrast, in CMC-free systems (MEI and MEII), these changes exceeded 20%, highlighting the crucial role of CMC in maintaining emulsion integrity.

Encapsulation efficiency declined most notably for selenium (hydrophilic agent encapsulated in the internal droplets), with reductions of  $\sim 24\%$  in MEI and  $\sim 31\%$  in MEII (emulsions without CMC) compared to the initial value. The emulsions with 0.3–0.5 wt.% CMC showed minimal losses ( $< 3.5\%$ ). Similar trends were observed for resveratrol (lipophilic agent encapsulated in the membrane phase drops), with  $\sim 10\%$  losses in CMC-free emulsions. These findings confirm that CMC significantly enhances emulsion stability, preserving droplet structure and active compound retention.

### 3.2.2. Oxidative stability of emulsified oil

The acid profile of sesame oil in the emulsion was analysed as a key indicator of its chemical stability. The fatty acid profiles in free and emulsified sesame oil (extracted from MEI-CMC(0.3)) over 90 days of storage are presented in Table 4. This formulation was selected as a representative system due to its intermediate CMC concentration and good stability observed during storage.

The results showed an increase in saturated fatty acids (SFA) content over the storage period in free sesame oil (13.70  $\rightarrow$  14.10%) and extracted oil (14.31  $\rightarrow$  14.90%). This may be attributed to the slightly oxidative degradation of unsaturated fatty acids over time, a well-documented phenomenon in stored oils. MUFAs remained relatively stable in free sesame oil, with only marginal differences observed (39.70  $\rightarrow$  39.37%). In the emulsified oil, a slight increase in MUFAs was noted (39.83  $\rightarrow$  40.04%), potentially due to the protective effects of the emulsion system stabilised by CMC. PUFAs, including linoleic acid (C18:2), demonstrated remarkable stability during the storage period in both sesame oil forms. The values for PUFAs hovered around 41% across all conditions, indicating resistance to oxidative degradation. This stability aligns with findings from research on sesame oil, which contains natural antioxidants such as sesamol and sesamin that help protect unsaturated fatty acids during storage (Namiki, 2007). Emulsified oils, in particular, may benefit from these antioxidant effects, as the emulsified structure can provide an additional barrier against oxidation (McClements and Decker, 2000).

These results highlight the enhanced stability of emulsified oil compared to non-emulsified oil, thanks to the presence of natural antioxidants (sesame oil ingredients: sesamol and sesamin) and the presence of stabilising components like CMC. Although CMC itself is not an antioxidant, it can indirectly reduce oxidation. A viscous layer around the oil droplets formed by CMC may limit oxygen access, thereby slowing lipid oxidation.

### 3.3. Impact of gastric conditions

Gastric acidity and enzymatic activity significantly affect emulsion stability and drug absorption (Gavhane and Yadav, 2012; Tan et al., 2020). Gastric retention time depends on droplet size, composition, and viscosity (Hamad et al., 2022; Salvia-Trujillo et al., 2013). Smaller droplets generally empty the stomach faster due to liquid-like behaviour and higher susceptibility to enzymatic action. However, increased viscosity can markedly slow gastric emptying, extending retention times by forming more cohesive, structured systems that resist flow. Larger droplets, especially when combined with higher viscosity in the continuous phase, tend to exhibit behaviour similar to semi-solid foods, with prolonged retention times. Consequently, both droplet size and rheological properties are critical parameters in designing emulsions for targeted delivery within the gastrointestinal tract.

#### 3.3.1. Droplet size changes under gastric conditions

Figures 4A and 4B show changes in droplet size distribution and Sauter diameter over 3 hours in simulated gastric conditions (pH 2, SGF).

After one hour of exposure, droplet size and distribution changes were negligible for emulsions containing CMC, demonstrating its protective effect during short gastric residence. After 3 hours, Set I emulsions (smaller droplets,  $\sim 10\ \mu\text{m}$ ) exhibited greater stability, particularly with 0.3 and 0.5 wt.% CMC, where droplet size distributions remained narrow and stable. In contrast, the absence of CMC (MEI) led to significant droplet growth and a shift towards a bimodal distribution, indicating coalescence and destabilisation. Set II emulsions (larger droplets,  $\sim 20\ \mu\text{m}$ ) were more prone to droplet growth, especially without CMC, with sizes increasing from  $\sim 25$  to  $\sim 43\ \mu\text{m}$  after 3 hours. Low CMC concentrations (0.1 wt.%) reduced but did not prevent coalescence, while 0.5 wt.% CMC provided effective protection by increasing viscosity and forming a stabilising polymer network (Figure 2B).

The results confirmed the key role of CMC in maintaining emulsion stability and supporting its use in controlled-release systems. These results also highlighted that gastric retention time strongly influences carrier stability, demonstrating that residence time and formulation parameters are critical factors in designing effective delivery systems.



### 3.3.2. $\zeta$ -potential analysis of emulsions in simulated gastric conditions

Figure 4C displays the  $\zeta$ -potential changes of CMC-stabilised emulsions under simulated gastric conditions (pH 2), compared to neutral pH (pH 7), over 1, 2, and 3 hours. At pH 7, all emulsions exhibited strongly negative  $\zeta$ -potential values, particularly those containing higher concentrations of carboxymethyl cellulose (CMC). For example, MEI-CMC(0.5) and MEII-CMC(0.5) recorded initial values around  $-50$  mV, indicative of effective electrostatic stabilisation arising from the complete dissociation (ionisation) of carboxyl groups. This high surface charge promotes strong repulsion between droplets, thus maintaining emulsion stability and preventing coalescence (Wang and Yi, 2023). Furthermore,  $\zeta$ -potential values remained relatively stable over the 3-hour period at neutral pH, with fluctuations below 10%, suggesting good interfacial robustness in non-acidic environments.

Under acidic conditions (pH 2), by contrast, a marked shift towards less negative  $\zeta$ -potential values was observed across all formulations. This decrease, down to approximately  $-25$  to  $-30$  mV in emulsions with 0.5 wt.% CMC, can be attributed to protonation of CMC's carboxyl groups, which reduces their net charge and weakens electrostatic repulsion. The pH-sensitive behaviour of CMC thus leads to diminished surface charge and, potentially, reduced colloidal stability. Nevertheless, high-CMC systems retained a comparatively negative  $\zeta$ -potential even

after 3 hours of exposure, suggesting partial preservation of interfacial charge. This may be due to incomplete protonation, as well as the presence of co-emulsifiers (e.g. Tween 80, Pluronic P-123), which could reinforce the interfacial structure through steric effects or hydrogen bonding.

The  $\zeta$ -potential data confirm that both pH and CMC content play a critical role in determining interfacial characteristics. The transition to a less charged but still cohesive interfacial layer at low pH supports the hypothesis that emulsions undergo interfacial compaction under gastric conditions, which may contribute to their resistance to coalescence and improved physical stability during gastric transit.

### 3.3.3. Release profiles of chemopreventive agents

Multiple emulsions (Sets I and II) were evaluated for their ability to minimise compound loss during gastric transit. Release profiles of chemopreventive agents were monitored over three hours in simulated gastric fluid (SGF) (Figure 5).

Release varied markedly across emulsions due to the combined effects of CMC content and droplet size. After 3 hours in SGF, CMC-free systems exhibited the highest release: MEI reached 100% for both resveratrol and selenium, while MEII released  $\sim 88\%$  and  $\sim 98\%$ , respectively. However, the most substantial changes in release profiles occurred within the first two hours of gastric exposure. Emulsions containing

Table 4. Fatty acid profile (%) in free and emulsified sesame oil during storage (90 days). Values are presented as a means of measurement: mean  $\pm$  SD ( $n = 3$ ).

Time of storage $\rightarrow$	0 days	90 days	0 days	90 days
Fatty acids	Free sesame oil		Sesame oil extracted from emulsion MEI-CMC(0.3)	
C16:0	8.90 <sup>a</sup> $\pm$ 0.17	10.01 <sup>b</sup> $\pm$ 0.01	9.46 <sup>c</sup> $\pm$ 0.05	9.99 <sup>c</sup> $\pm$ 0.49
C18:0	4.80 <sup>a</sup> $\pm$ 0.10	4.09 <sup>b</sup> $\pm$ 0.05	4.85 <sup>a</sup> $\pm$ 0.07	4.83 <sup>a</sup> $\pm$ 0.19
SFA	13.70 <sup>a</sup> $\pm$ 0.27	14.10 <sup>b</sup> $\pm$ 0.06	14.31 <sup>c</sup> $\pm$ 0.12	14.82 <sup>c</sup> $\pm$ 0.68
C16:1	0.20 <sup>a</sup> $\pm$ 0.00	0.05 <sup>b</sup> $\pm$ 0.01	0.20 <sup>a</sup> $\pm$ 0.01	0.18 <sup>c</sup> $\pm$ 0.03
C18:1	39.30 $\pm$ 0.39	39.27 $\pm$ 0.10	39.45 $\pm$ 0.07	39.75 $\pm$ 0.20
C20:1	0.20 <sup>a</sup> $\pm$ 0.00	0.05 <sup>b</sup> $\pm$ 0.01	0.18 <sup>a</sup> $\pm$ 0.02	0.10 <sup>c</sup> $\pm$ 0.00
MUFA	39.70 <sup>ab</sup> $\pm$ 0.39	39.37 <sup>a</sup> $\pm$ 0.12	39.83 <sup>b</sup> $\pm$ 0.10	40.03 <sup>b</sup> $\pm$ 0.23
C18:2	41.30 $\pm$ 0.41	41.13 $\pm$ 0.01	41.10 $\pm$ 0.14	41.24 $\pm$ 0.28
C18:3	0.30 <sup>a</sup> $\pm$ 0.01	0.05 <sup>b</sup> $\pm$ 0.01	0.21 <sup>c</sup> $\pm$ 0.01	0.08 <sup>d</sup> $\pm$ 0.01
PUFA	41.60 $\pm$ 0.42	41.18 $\pm$ 0.02	41.31 $\pm$ 0.15	41.32 $\pm$ 0.29

SFA-saturated fatty acids; MUFA-monounsaturated fatty acids; PUFA-polyunsaturated fatty acids. The values within the same row that share the same letter are not significantly different ( $p < 0.05$ ), while different letters indicate statistically significant differences based on one-way ANOVA followed by Tukey's HSD test.

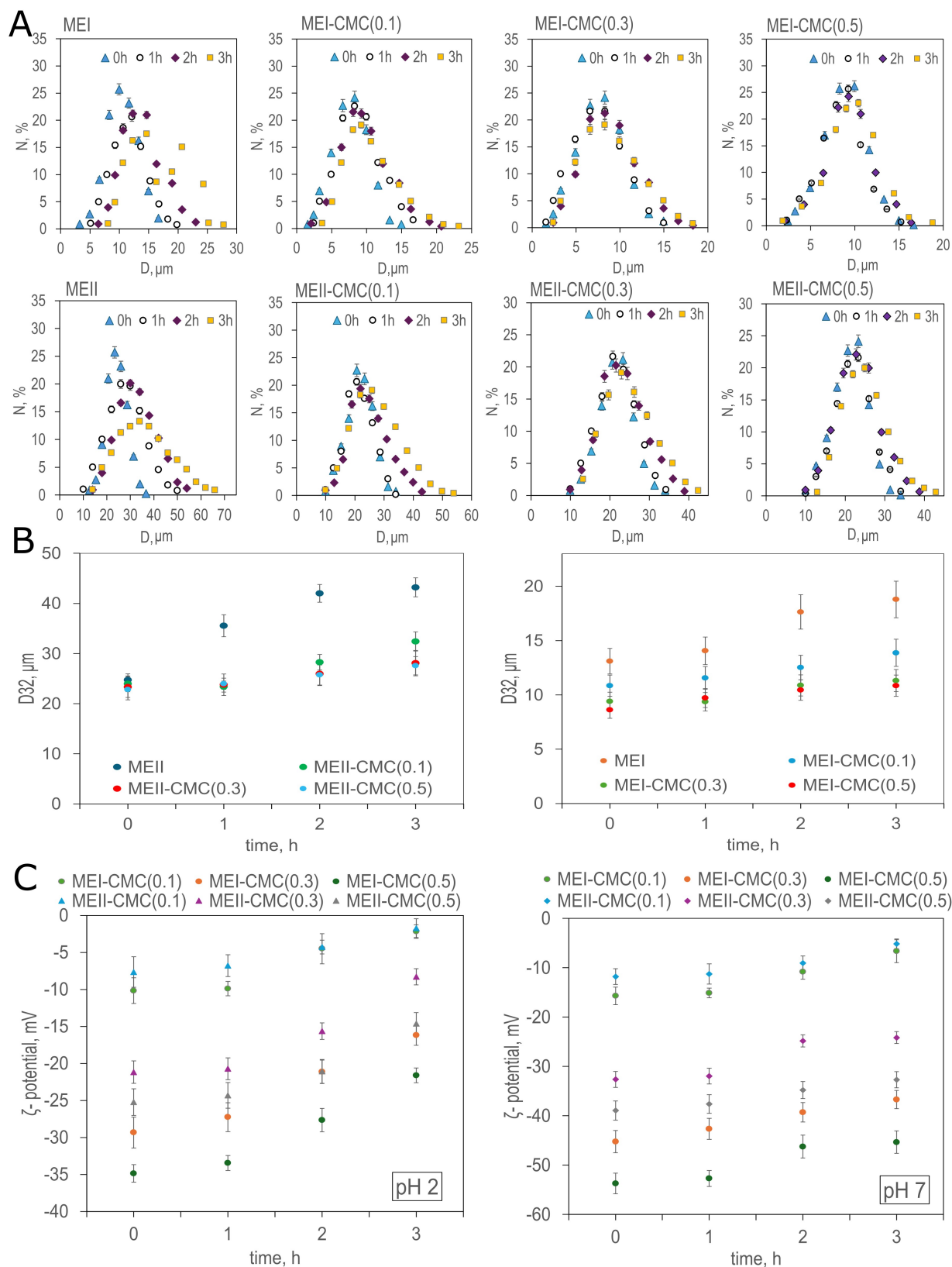


Figure 4. Changes in (A) the drop size distribution, (B) the drop diameter (D32-Sauter mean diameter of the membrane phase drops), and (C) zeta potential of multiple emulsions under simulated gastric conditions over varying residence times (0–3 h). Each value represents the *mean*  $\pm$  SD ( $n=3$ ).

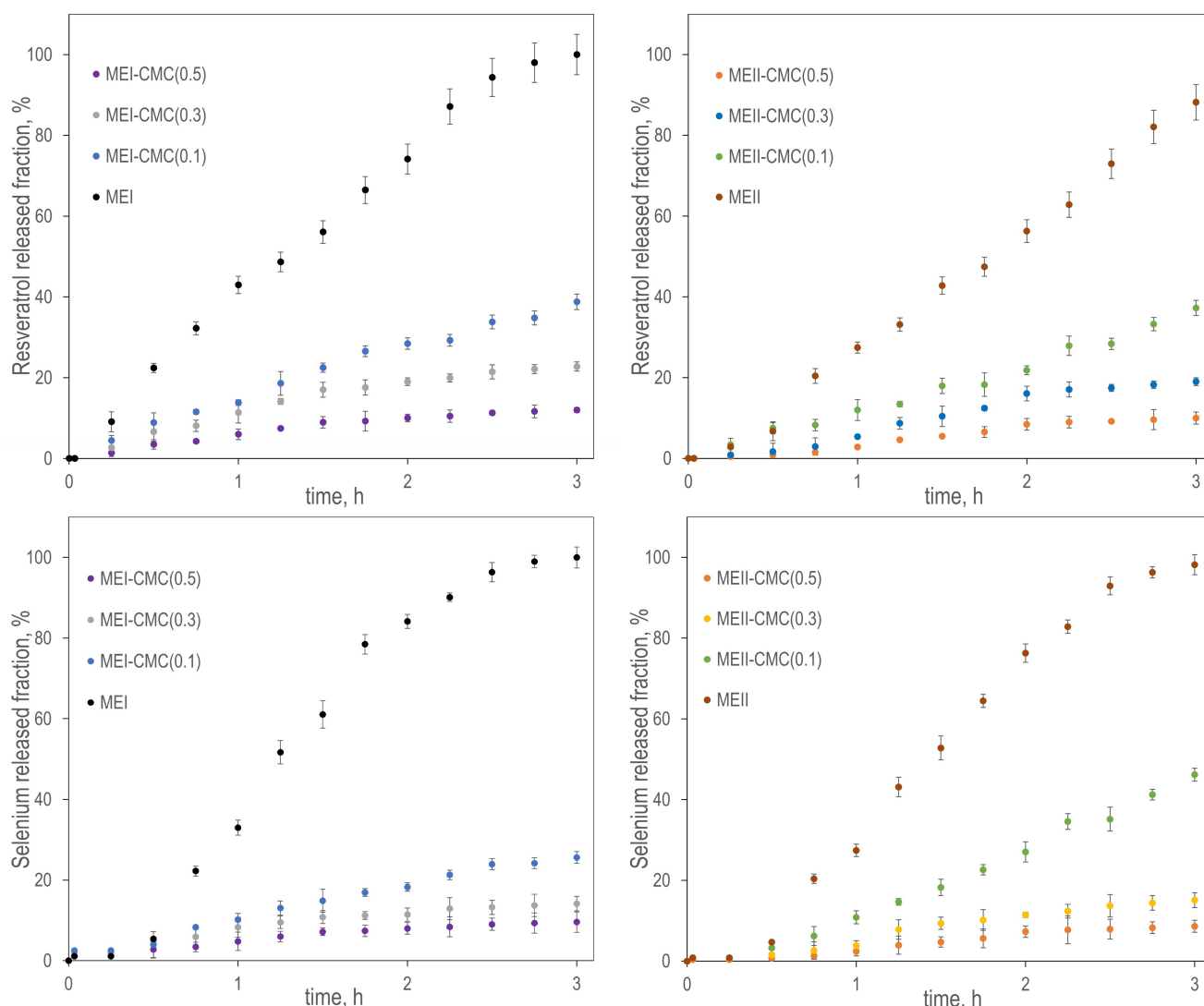


Figure 5. Effect of sodium carboxymethyl cellulose (CMC) content in emulsion on the release profiles of resveratrol and selenium under simulated gastric conditions (pH 2, presence of digestive enzymes). Each value represents  $mean \pm SD$  ( $n = 3$ ).

0.5 wt.% CMC significantly suppressed compound release; MEI-CMC(0.5) released only  $\sim 12\%$  resveratrol and  $\sim 9.6\%$  selenium, while MEII-CMC(0.5) reached  $\sim 10\%$  and  $\sim 8.6\%$ , respectively. Emulsions with 0.1–0.3 wt.% CMC showed intermediate release behaviour, following a clear concentration-dependent trend. Set I emulsions showed faster release than Set II at each CMC level, likely due to their smaller droplet size ( $\sim 10 \mu\text{m}$ ), higher surface area, and potentially denser polymer (CMC) interfacial coverage.

The controlled release observed in high-CMC emulsions confirms the role of CMC in forming an interfacial diffusion barrier. This effect was more pronounced for selenium, whose release was consistently slower, likely due to its localisation in internal droplets and possibly interactions with CMC (e.g. enhanced hydrogen bonding and electrostatic attraction) or other emulsion components (e.g. Pluronic P-123, Tween 80, sesame oil) (Nithya Priya et al., 2025). Overall, the results

indicate that combining smaller droplets with higher CMC concentrations allows for precise modulation (delaying) of release kinetics, critical for protecting chemopreventive agents during gastric transit and enhancing their delivery to the intestinal absorption site.

## 4. CONCLUSIONS

This study demonstrates that the droplet architecture of multiple emulsions, combined with the functional properties of sodium carboxymethyl cellulose (CMC), is critical in designing effective delivery systems for chemopreventive compounds in functional foods. CMC significantly enhanced droplet integrity, encapsulation efficiency, and oxidative stability, and controlled hydrophilic and lipophilic bioactive release profiles under simulated gastrointestinal conditions. These improvements contributed to delayed gastric release and improved

intestinal targeting, which are crucial for optimising the functional performance of the delivery system. By tuning the interfacial properties through CMC incorporation and controlling droplet structure via Couette–Taylor flow emulsification, this system offers a promising strategy for controlling release kinetics in functional delivery systems. Additionally, the use of food-grade components such as sesame oil, gelatin, and CMC, along with the compatibility of the production method with scalable processing systems, enhances the formulation's applicability for industrial food production. These results underscore the value of structural and interfacial design in developing food-grade multiple emulsions and position CMC as a multifunctional hydrocolloid capable of controlling emulsion behaviour across various stages of gastrointestinal transit. Moreover, the compositional flexibility of the emulsions facilitates their incorporation into a range of functional food products, including ready-to-drink beverages, fortified yoghurts, and nutraceutical supplements, supporting the advancement of consumer-friendly and health-promoting delivery platforms.

## SYMBOLS

$M_t$	a mass of the non-encapsulated compound in the external phase at a given time, g
$M_0$	an initial compound mass added to the emulsion during preparation, g
$D_{32}$	the Sauter diameter of the membrane phase drops, $\mu\text{m}$
$d_{32}$	the Sauter diameter of the internal phase droplets, $\mu\text{m}$
$EER$	the encapsulation efficiency of trans-resveratrol, %
$EES$	the encapsulation efficiency of selenium, %
<i>Greek symbols</i>	
$\zeta$	zeta potential, mV
$\mu$	apparent viscosity, mPa·s

## REFERENCES

- Ashique S., Bhowmick M., Pal R., Khatoon H., Kumar P., Sharma H., Garg A., Kumar S., Das U., 2024. Multi-drug resistance in Colorectal Cancer – approaches to overcome, advancements and future success. *Adv. Cancer Biol. – Metastasis*, 10, 100114. DOI: [10.1016/j.adcanc.2024.100114](https://doi.org/10.1016/j.adcanc.2024.100114).
- Benchabane A., Bekkour K., 2008. Rheological properties of carboxymethyl cellulose (CMC) solutions. *Colloid. Polym. Sci.*, 286, 1173–1180. DOI: [10.1007/s00396-008-1882-2](https://doi.org/10.1007/s00396-008-1882-2).
- Bera B.C., Chakrabartty M.M., 1968. Spectrophotometric determination of selenium with 2-mercaptobenzothiazole. *Analyst*, 93, 50–55. DOI: [10.1039/an9689300050](https://doi.org/10.1039/an9689300050).
- Camont L., Cottart C.H., Rhayem Y., Nivet-Antoine V., Djelidi R., Collin F., Beaudeau J.L., Bonnefont-Rousselot D., 2009. Simple spectrophotometric assessment of the trans-/cis-resveratrol ratio in aqueous solutions. *Anal. Chim. Acta*, 634, 121–128. DOI: [10.1016/j.aca.2008.12.003](https://doi.org/10.1016/j.aca.2008.12.003).
- Cook S.L., Woods S., Methven L., Parker J.K., Khutoryanskiy V.V., 2018. Mucoadhesive polysaccharides modulate sodium retention, release and taste perception. *Food Chem.*, 240, 482–489. DOI: [10.1016/j.foodchem.2017.07.134](https://doi.org/10.1016/j.foodchem.2017.07.134).
- Dluska E., Markowska-Radomska A., Metera A., Rudniak L., Kosicki K., 2022. Mass transfer of anti-cancer drug delivery to brain tumours by a multiple emulsion-based implant. *AIChE J.*, 68, e17501. DOI: [10.1002/aic.17501](https://doi.org/10.1002/aic.17501).
- Dluska E., Markowska-Radomska A., Metera A., Tudek B., Kosicki K., 2017. Multiple emulsions as effective platforms for controlled anti-cancer drug delivery. *Nanomedicine*, 12, 2183–2197. DOI: [10.2217/nnm-2017-0112](https://doi.org/10.2217/nnm-2017-0112).
- Dluska E., Metera A., Markowska-Radomska A., Tudek B., 2019. Effective cryopreservation and recovery of living cells encapsulated in multiple emulsions. *Biopreserv. Biobanking*, 17, 468–476. DOI: [10.1089/bio.2018.0134](https://doi.org/10.1089/bio.2018.0134).
- Fathi M., Vinceković M., Jurić S., Viskić M., Režek Jambrak A., Donsi F., 2019. Food-grade colloidal systems for the delivery of essential oils. *Food Rev. Int.*, 37, 1–45. DOI: [10.1080/87559129.2019.1687514](https://doi.org/10.1080/87559129.2019.1687514).
- Folch J., Lees M., Sloane Stanley G.H., 1957. A simple method for the isolation and purification of total lipides from animal tissues. *J. Biol. Chem.*, 226, 497–509. DOI: [10.1016/S0021-9258\(18\)64849-5](https://doi.org/10.1016/S0021-9258(18)64849-5).
- Gavhane Y.N., Yadav A.V., 2012. Loss of orally administered drugs in GI tract. *Saudi Pharm. J.*, 20, 331–344. DOI: [10.1016/j.jsps.2012.03.005](https://doi.org/10.1016/j.jsps.2012.03.005).
- Hamad S., Chen R., Zhou Z., Nasr P., Li Y.L., Rafiee Tari N., Rogers M.A., Wright A.J., 2022. Palm lipid emulsion droplet crystallinity and gastric acid stability in relation to *in vitro* bioaccessibility and *in vivo* gastric emptying. *Front. Nutr.*, 9, 940045. DOI: [10.3389/fnut.2022.940045](https://doi.org/10.3389/fnut.2022.940045).
- Huang J., Chen X., Su D., Chen L., Chen C., Jin B., 2023. Molecular mechanisms affecting the stability of high internal phase emulsions of zein–soy isoflavone complexes fabricated with ultrasound-assisted dynamic high-pressure microfluidization. *Food Res. Int.*, 170, 113051. DOI: [10.1016/j.foodres.2023.113051](https://doi.org/10.1016/j.foodres.2023.113051).
- Islam M.R., Rauf A., Akash S., Trisha S.I., Nasim A.H., Akter M., Dhar P.S., Ogaly H.A., Hemeg H.A., Wilairatana P., Muthu T., 2024. Targeted therapies of curcumin focus on its therapeutic benefits in cancers and human health: Molecular signaling pathway-based approaches and future perspectives. *Biomed. Pharmacother.*, 170, 116034. DOI: [10.1016/j.biopha.2023.116034](https://doi.org/10.1016/j.biopha.2023.116034).
- Jia X., Xu R., Shen W., Xie M., Abid M., Jabbar S., Wang P., Zeng X., Wu T., 2015. Stabilizing oil-in-water emulsion with amorphous cellulose. *Food Hydrocolloids*, 43, 275–282. DOI: [10.1016/j.foodhyd.2014.05.024](https://doi.org/10.1016/j.foodhyd.2014.05.024).
- Katona B.W., Weiss J.M., 2020. Chemoprevention of colorectal cancer. *Gastroenterology*, 158, 368–388. DOI: [10.1053/j.gastro.2019.06.047](https://doi.org/10.1053/j.gastro.2019.06.047).
- Lavoisier A., Shreeram S., Jedwab M., Ramaioli M., 2021. Effect of the rheological properties of the liquid carrier on the *in vitro* swallowing of solid oral dosage forms. *J. Texture Stud.*, 52, 623–637. DOI: [10.1111/jtxs.12618](https://doi.org/10.1111/jtxs.12618).



- Li W., Liu D., Song L., Li H., Dai S., Su Y., Li Q., Li J., Zheng T., 2022. Surface modified porous silicon with chitosan coating as a pH-responsive controlled delivery system for lutein. *Food Funct.*, 13, 6129–6138. DOI: [10.1039/D2FO00101B](https://doi.org/10.1039/D2FO00101B).
- Li Y., Pei Y., Shan Z., Jiang Y., Cui S.W., He Z., Zhang Y., Wang H., 2024. A pH-sensitive W/O/W emulsion-bound carboxymethyl chitosan–alginate hydrogel bead system through the Maillard reaction for probiotics intestine-targeted delivery. *Food Hydrocolloids*, 153, 109956. DOI: [10.1016/j.foodhyd.2024.109956](https://doi.org/10.1016/j.foodhyd.2024.109956).
- Liu Y., Liang Y., Yuhong J., Xin P., Han J.L., Du Y., Yu X., Zhu R., Zhang M., Chen W., Ma Y., 2024. Advances in nanotechnology for enhancing the solubility and bioavailability of poorly soluble drugs. *Drug Des. Devel. Ther.*, 18, 1469–1495. DOI: [10.2147/DDDT.S447496](https://doi.org/10.2147/DDDT.S447496).
- Lu H., Zhang S., Wang J., Chen Q., 2021. A review on polymer and lipid-based nanocarriers and its application to nanopharmaeaceutical and food-based systems. *Front. Nutr.*, 8, 783831. DOI: [10.3389/fnut.2021.783831](https://doi.org/10.3389/fnut.2021.783831).
- Lu W., Kelly A.L., Miao S., 2016. Emulsion-based encapsulation and delivery systems for polyphenols. *Trends Food Sci. Technol.*, 47, 1–9. DOI: [10.1016/j.tifs.2015.10.015](https://doi.org/10.1016/j.tifs.2015.10.015).
- Majumdar A.P.N., Banerjee S., Nautiyal J., Patel B.B., Patel V., Du J., Yu Y., Elliott A.A., Levi E., Sarkar F.H., 2009. Curcumin synergizes with resveratrol to inhibit colon cancer. *Nutri. Cancer*, 61, 544–553. DOI: [10.1080/01635580902752262](https://doi.org/10.1080/01635580902752262).
- Mall J., Naseem N., Haider M.F., Rahman M.A., Khan S., Siddiqui S.N., 2025. Nanostructured lipid carriers as a drug delivery system: A comprehensive review with therapeutic applications. *Intell. Pharm.*, 3, 243–255. DOI: [10.1016/j.ipha.2024.09.005](https://doi.org/10.1016/j.ipha.2024.09.005).
- Markowska-Radomska A., Dluska E., 2012. The multiple emulsion entrapping active agent produced via one-step preparation method in the liquid-liquid helical flow for drug release study and modeling. In: Starov V., Griffiths P. (Eds.), *UK Colloids 2011. Progress in Colloid and Polymer Science*, 139, 29–34. Springer, Berlin, Heidelberg. DOI: [10.1007/978-3-642-28974-3\\_6](https://doi.org/10.1007/978-3-642-28974-3_6).
- Markowska-Radomska A., Dluska E., Metera A., Wojcieszak M., 2021. Multiple emulsions for simultaneous active agents delivery in a skin topical application. *Chem. Proc. Eng.*, 42(3), 263–273. DOI: [10.24425/cpe.2021.138930](https://doi.org/10.24425/cpe.2021.138930).
- McClements D.J., Decker E.A., 2000. Lipid oxidation in oil-in-water emulsions: Impact of molecular environment on chemical reactions in heterogeneous food system. *J. Food Sci.*, 65, 1270–1282. DOI: [10.1111/j.1365-2621.2000.tb10596.x](https://doi.org/10.1111/j.1365-2621.2000.tb10596.x).
- McClements D.J., Decker E.A., Weiss J., 2007. Emulsion-based delivery systems for lipophilic bioactive components. *J. Food Sci.*, 72, R109–R124. DOI: [10.1111/j.1750-3841.2007.00507.x](https://doi.org/10.1111/j.1750-3841.2007.00507.x).
- Minekus M., Alminger M., Alvito P., Ballance S., Bohn T., Bourlieu C., Carrière F., Boutrou R., Corredig M., Dupont D., Dufour C., Egger L., Golding M., Karakaya S., Kirkhus B., Le Feunteun S., Lesmes U., Macierzanka A., Mackie A., Marze S., McClements D.J., Ménard O., Recio I., Santos C.N., Singh R.P., Vegarud G.E., Wickham M.S., Weitschies W., Brodtkorb A., 2014. A standardised static in vitro digestion method suitable for food – an international consensus. *Food Funct.*, 5, 1113–1124. DOI: [10.1039/c3fo60702j](https://doi.org/10.1039/c3fo60702j).
- Namiki M., 2007. Nutraceutical functions of sesame: A review. *Crit. Rev. Food Sci. Nutr.*, 47, 651–673. DOI: [10.1080/10408390600919114](https://doi.org/10.1080/10408390600919114).
- Nithya Priya V., Rajkumar M., Rajendran V., Mobika J., Linto Sibi S.P., Veena B., Vijayalakshmi V., Ahila P., 2025. Sustainable selenium ions adsorption of cyclodextrin and cellulose functionalized layered double hydroxide/reduced graphene oxide nanocomposites. *J. Water Process Eng.*, 69, 106580. DOI: [10.1016/j.jwpe.2024.106580](https://doi.org/10.1016/j.jwpe.2024.106580).
- Salvia-Trujillo L., Qian C., Martin-Belloso O., McClements D.J., 2013. Influence of particle size on lipid digestion and beta-carotene bioaccessibility in emulsions and nanoemulsions. *Food Chem.*, 141, 1472–1480. DOI: [10.1016/j.foodchem.2013.03.050](https://doi.org/10.1016/j.foodchem.2013.03.050).
- Sheng Y., Gao J., Yin Z.Z., Kang J., Kong Y., 2021. Dual-drug delivery system based on the hydrogels of alginate and sodium carboxymethyl cellulose for colorectal cancer treatment. *Carbohydr. Polym.*, 269, 118325. DOI: [10.1016/j.carbpol.2021.118325](https://doi.org/10.1016/j.carbpol.2021.118325).
- Suñer J., Calpena A.C., Clares B., Cañadas C., Halbaut L., 2017. Development of clotrimazole multiple W/O/W emulsions as vehicles for drug delivery: effects of additives on emulsion stability. *AAPS PharmSciTech.*, 18, 539–550. DOI: [10.1208/s12249-016-0529-8](https://doi.org/10.1208/s12249-016-0529-8).
- Tan Y., Zhang Z., Muriel Mundo J., McClements D.J., 2020. Factors impacting lipid digestion and nutraceutical bioaccessibility assessed by standardized gastrointestinal model (INFOGEST): Emulsifier type. *Food Res. Inter.*, 137, 109739. DOI: [10.1016/j.foodres.2020.109739](https://doi.org/10.1016/j.foodres.2020.109739).
- Wang L.Y., Zhao S., Lv G.-J., Ma X.-J., Zhang J.-B., 2020. Mechanisms of resveratrol in the prevention and treatment of gastrointestinal cancer. *World J. Clin. Cases*, 8, 2425–2437. DOI: [10.12998/wjcc.v8.i12.2425](https://doi.org/10.12998/wjcc.v8.i12.2425).
- Wang R., Yi H., 2023. Mechanical-induced functionalization of graphene with sodium carboxymethyl cellulose toward enhancing anticorrosion performance of waterborne epoxy coatings. *J. Coat. Technol. Res.*, 20, 2069–2080. DOI: [10.1007/s11998-023-00802-6](https://doi.org/10.1007/s11998-023-00802-6).
- Wang W., Ji S., Xia Q., 2024. Influence of carboxymethyl cellulose on the stability, rheology, and curcumin bioaccessibility of high internal phase Pickering emulsions. *Carbohydr. Polym.*, 334, 122041. DOI: [10.1016/j.carbpol.2024.122041](https://doi.org/10.1016/j.carbpol.2024.122041).
- Wang Z., Song X.-Q., Xu W., Lei S., Zhang H., Yang L., 2023. Stand up to stand out: Natural dietary polyphenols curcumin, resveratrol, and gossypol as potential therapeutic candidates against severe acute respiratory syndrome coronavirus 2 infection. *Nutrients*, 15, 3885. DOI: [10.3390/nu15183885](https://doi.org/10.3390/nu15183885).
- Zhuang Y., Li L., Feng L., Wang S., Su H., Liu H., Liu H., Wu Y., 2020. Mitochondrion-targeted selenium nanoparticles enhance reactive oxygen species-mediated cell death. *Nanoscale*, 12, 1389–1396. DOI: [10.1039/C9NR909039H](https://doi.org/10.1039/C9NR909039H).